主論文（雑誌掲載版）

JOURNAL OF TISSUE ENGINEERING AND REGENERATIVE MEDICINE
J Tissue Eng Regen Med (2015)
Published online in Wiley Online Library (wileyonlinelibrary.com) **DOI:** 10.1002/term.2060

RESEARCH ARTICLE

The efficacy of a novel collagen–gelatin scaffold with basic fibroblast growth factor for the treatment of vocal fold scar

Nao Hiwatashi[1], Shigeru Hirano[1]*, Masanobu Mizuta[1,2], Toshiki Kobayashi[3], Yoshitaka Kawai[1], Shin-ichi Kanemaru[1,4], Tatsuo Nakamura[5], Juichi Ito[1], Katsuya Kawai[6] and Shigehiko Suzuki[6]

[1]*Department of Otolaryngology–Head and Neck Surgery, Graduate School of Medicine, Kyoto University, Japan*
[2]*Department of Otolaryngology, Vanderbilt University, Nashville, TN, USA*
[3]*Department of Otorhinolaryngology, Jikei University of Medicine, Tokyo, Japan*
[4]*Department of Otolaryngology–Head and Neck Surgery, Kitano Hospital, Tazuke Kofukai Medical Research Institute, Osaka, Japan*
[5]*Department of Bioartificial Organs, Institute for Frontier Medical Science, Kyoto University, Japan*
[6]*Department of Plastic and Reconstructive Surgery, Graduate School of Medicine, Kyoto University, Japan*

Abstract

Vocal fold scar remains a therapeutic challenge. Basic fibroblast growth factor (bFGF) was reported to have regenerative effects for vocal fold scar, although it has the disadvantage of rapid absorption *in vivo*. A collagen–gelatin sponge (CGS) can compensate for the disadvantage by providing a sustained release system. The current study evaluated the efficacy of CGS combined with bFGF on vocal fold scar, using rat fibroblasts for an *in vitro* model and a canine *in vivo* model. We prepared fibroblasts from scarred vocal folds (sVFs) in rats and showed that bFGF accelerated cell proliferation and suppressed expression levels of cleaved caspase 3 and α-smooth muscle actin. *Has 1*, *Has 3*, *Fgf2*, *Hgf* and *Vegfa* mRNA levels were significantly upregulated, while *Col1a1* and *Col3a1* were dose-dependently downregulated, with a maximum effect at 100 ng/ml bFGF. In an *in vivo* assay, 6 weeks after lamina propria stripping, beagles were divided into three groups: CGS alone (CGS group); CGS with bFGF (7 μg/cm^2; CGS + bFGF group); or a sham-treated group. Vibratory examination revealed that the glottal gap was significantly reduced in the bFGF group and the two implanted groups, whereas the CGS + bFGF group showed higher mucosal wave amplitude. Histological examination revealed significantly restored hyaluronic acid and elastin redistribution in the CGS + bFGF group and reductions in dense collagen deposition. These results provide evidence that CGS and bFGF combination therapy may have therapeutic potential and could be a promising tool for treating vocal fold scar. Copyright © 2015 John Wiley & Sons, Ltd.

Received 13 August 2014; Revised 26 February 2015; Accepted 29 April 2015

Keywords **vocal fold scar; collagen–gelatin sponge; basic fibroblast growth factor; myofibroblast; scaffold; regeneration**

1. Introduction

The normal vocal fold is composed of epithelium, the lamina propria (LP) and underlying muscle. Human vocal folds have a unique tri-layered LP, composed of superficial, intermediate and deep layers. Each layer is characterized by major extracellular matrix (ECM) components, various proteoglycans and glycosaminoglycans in the superficial layer, elastin in the intermediate layer and collagen in the deep layer (Hirano, 1974). It is indispensable for producing the normal voice that non-contractile and soft tissue, consisting of the epithelium, superficial and intermediate layers, show pliable oscillation during phonation.

Vocal fold scar occurs after phonotrauma or inflammation as well as clinical treatments such as surgery or radiotherapy. Such scarring causes a loss of vocal fold pliability

**Correspondence to: Shigeru. Hirano, Department of Otolaryngology–Head and Neck Surgery, Graduate School of Medicine, Kyoto University, Sakyo-ku, Kyoto 606-8507, Japan. E-mail: hirano@ent.kuhp.kyoto-u.ac.jp*

Copyright © 2015 John Wiley & Sons, Ltd.

and a marked decrease in vibration of the mucosa (Hirano, 2005) and can subsequently cause a decrease in the quality of life, due to hoarseness or a weak voice. According to previous research, vocal fold scar presents with histological changes, such as excessive collagen deposition, disorganized elastin or decorin and occasional decreases in hyaluronic acid (HA) (Hirano *et al*., 2009; Rousseau *et al*., 2003, 2004; Tateya *et al*., 2005). These changes cause contraction of the vocal fold, leading to increased stiffness and glottal insufficiency. Advancements in phonosurgery have resolved most vocal fold pathologies, whereas vocal fold scar that is resistant to conventional therapies continues to be a therapeutic issue in the management of vocal fold scar.

Fibroblasts play a central role in the wound-healing process that occurs in injured vocal folds. However, during wound healing some fibroblasts are induced to change their phenotype to become α-smooth muscle actin (αSMA)-expressing myofibroblasts (Desmouliere, 1995). These myofibroblasts are reported to be related to tissue contraction and can secrete excessive amounts of type I collagen. Despite the importance of understanding the biological features of myofibroblasts in the management of vocal fold scar, to date few reports have investigated the role of fibroblasts and myofibroblasts in scarred vocal folds. Thus, further insight into the behaviour of scarred vocal fold fibroblasts (sVFs) *in vitro* is required to better determine their behaviour *in vivo*.

Basic fibroblast growth factor (bFGF) was identified in 1974 as a strong inducer of proliferation and fibroblast migration, and was also shown to promote capillary formation and accelerate tissue regeneration (Gospodarowicz, 1974; McGee *et al*., 1988). Our previous *in vivo* studies demonstrated that local injection of bFGF could restore scarred vocal folds. Histological examination following bFGF treatment revealed an increase in HA and a reduction in collagen deposition that led to functional vibratory improvement (Suehiro *et al*., 2010). Despite its effectiveness, bFGF has the disadvantage of having a very short half-life, due to its rapid absorption *in vivo*. Isogai *et al*. (2005) reported that approximately 97% of bFGF disappeared within 1 day after injection into the subcutaneous space of mice. In clinical usage, local injections should be repeated several times in order to maintain appropriate concentrations at the target tissues.

To compensate for this disadvantage, carriers, especially scaffolds, that show sustained release of growth factors are needed for an effective drug-delivery system. As a novel scaffold, collagen–gelatin sponge (CGS) was developed from artificial dermis (Takemoto *et al*., 2008). This material is synthesized by adding gelatin during the manufacture of the collagen sponge. The collagen sponge acts as a temporary bed whereupon surrounding cells can infiltrate into the sponge pores and begin to synthesize new collagen fibres until they form regenerated connective tissue. bFGF binds to acidic gelatin through ionic interactions, and bFGF is gradually released during the biodegradation of the sponge (Tabata *et al*., 1999). Previous studies using CGS impregnated with bFGF for skin defects in mice or palatine membrane defects in beagles demonstrated the accelerated formation of dermis-like tissue and new capillaries (Ayvazyan *et al*., 2011; Kanda *et al*., 2012) and these studies were followed by a clinical trial for patients with chronic skin ulcers (Morimoto *et al*., 2013).

The combination of CGS and bFGF is a candidate tool for the treatment of vocal fold scar. The aim of this study was to evaluate the efficacy of the combination of CGS and bFGF for the treatment of vocal fold scar *in vivo*, with a focus on ECM restoration and functional recovery. Another aim was to analyse cell proliferation, apoptosis, α-SMA expression and gene expression of ECM components to clarify the mechanism by which bFGF affects sVF *in vitro*.

2. Materials and methods

2.1. Animals

In this study, six Sprague–Dawley transgenic (CAG–EGFP) rats, aged 13 weeks, and 15 beagles, weight 9–12 kg, were used for *in vitro* and *in vivo* assays, respectively. CAG–EGFP rats are chimeric rats that express enhanced green fluorescence protein (EGFP) throughout the body under the control of cytomegalovirus enhancer and the chicken β-actin promoter derived from an expression vector, pCAGGS. The expression of EGFP allowed us to track any progeny of the cultured cells from the chimeric rats, using green fluorescence as a tag (Ito *et al*., 2001). Animal care was conducted in the Institute of Laboratory Animals of the Graduate School of Medicine, Kyoto University. The number of animals used in this study was kept to a minimum. All possible efforts to reduce animal suffering were made and were in compliance with protocols established by the Animal Research Committee of Kyoto University.

2.2. Preparation of collagen–gelatin sponge

Collagen–gelatin sponge was manufactured as previously reported (Takemoto *et al*., 2008). Briefly, gelatin isolated from pig dermis with an isoelectric point (IEP) of 5.0 and a molecular weight of 99 000 (Nippi Inc., Osaka, Japan) and atelocollagen isolated from pig tendon with an IEP of 8.5 and a molecular weight of 300 000 (Nitta Gelatin Inc., Osaka, Japan) were used. A collagen and gelatin solution with a gelatin concentration of 10 wt% of the total solutes was prepared by mixing 3 wt% gelatin solution with 0.3 wt% collagen solution. The foamy solution was poured into a mould, frozen rapidly and freeze-dried. The collagen–gelatin sheet was crosslinked by immersion in 0.2% glutaraldehyde at 4 °C for 24 h and freeze-drying.

Copyright © 2015 John Wiley & Sons, Ltd.

DOI: 10.1002/term

2.3. Isolation and cell culture of scarred vocal fold fibroblasts

The rats were anaesthetized with an intraperitoneal injection of ketamine hydrochloride (60 mg/kg) and xylazine hydrochloride (6 mg/kg). Atropine sulphate (0.005 mg/kg) was also injected intraperitoneally to reduce the secretion of saliva and sputum in the laryngeal lumen. After placement of the animal on a custom-made operating platform, the larynges were visualized through an endoscope inserted transorally. The bilateral vocal folds were then stripped with microscissors until the thyroarytenoid muscle was exposed. Two months after the initial surgery, the rats were anaesthetized using the same procedures and the larynges were harvested. This surgical procedure and the time point for scar maturation was described previously (Tateya *et al*., 2005). Soon afterwards, we proceeded to the resection of the LP and epithelia of the vocal folds, which were minced into small pieces in 10 cm plastic plates under a dissecting microscope. The tissue was then cultured in basic medium consisting of Dulbecco's modified Eagle's medium (DMEM) supplemented with 10% fetal bovine serum (FBS) and antibiotics, at 37 °C with 5% carbon dioxide. The adherent 80% confluent cells were trypsinized and passaged before use at the second passage. These tissue-explant culture methods have been established and the cultured cells were characterized as sVF in line with the previous reports (Jette *et al*., 2013; Thibeault *et al*., 2008).

Suspensions of 1.0×10^4 cells in 10 µl DMEM were seeded onto $4 \times 4\,mm^2$ and 3 mm thick collagen–gelatin sponges in 24-well microplates, using a Hamilton syringe with a 26G needle. After cell starvation culture in DMEM–0.1% bovine serum albumin (BSA) for 24 h, the samples were washed with phosphate-buffered saline (PBS) and gently transferred onto new microplates, then DMEM-containing solutions of bFGF (Fibrast spray; Kaken Pharmaceutical, Tokyo, Japan) were added to paired wells adjusted to various final bFGF concentrations (0, 1, 10 and 100 ng/ml). Samples were used at the specified time points for each assay and the culture medium was not changed, which allowed bFGF levels to diminish naturally.

2.4. Cell proliferation assay

To compare the effects of bFGF on cell proliferation after cultivation for 1, 4, 7, 10 and 14 days, the number of sVFs on each CGS were counted. Cells were released from the CGS with 1% collagenase B (Roche Diagnostics GmbH, Mannheim, Germany) and counted using a haemocytometer (Bright-Line, Becton Dickinson, Franklin Lakes, NJ, USA). We counted the number of sVF from six samples for each bFGF condition at each time point.

2.5. Immunostaining

To evaluate the response of sVFs to bFGF, immunohistochemical analyses were performed using an antibody directed against cleaved caspase-3 (CC3) for an apoptosis assay and α-smooth muscle actin (αSMA) for detecting the myofibroblasts. After 7 days in culture, samples were fixed in 4% paraformaldehyde for 40 min and, after washing, were embedded in optimum cutting temperature (OCT) solution (Tissue-Tek, Kyoto, Japan) before freezing at –80 °C until use. Thereafter, 20 µm thick sections were placed onto microscope slides. The cells were permeabilized and blocked with a PBS solution containing 0.1% Triton-X and 5% normal goat serum. The samples were then incubated at 4 °C overnight with primary rabbit monoclonal antibodies against CC3 (1:50; Cell Signaling Technology, Danvers, MA, USA) and primary mouse monoclonal antibodies against αSMA (1:200; Sigma-Aldrich, St. Louis, MO, USA). The samples were washed and incubated for 1 h at room temperature in AlexaFluor 555 goat anti-rabbit IgG (1:100; Invitrogen, Carlsbad, CA, USA) or anti-mouse IgG (1:500; Invitrogen) secondary antibodies. Cell nuclei were stained with 4′,6-diamidino-2-phenylindole dihydrochloride (DAPI). For negative controls, the primary antibodies were omitted. Digital images were captured every 2 µm with a Leica TCS-SP2 laser-scanning confocal microscope (Leica Microsystems, Wetzlar, Germany). Section analysis was performed on 10 randomly chosen fields of $0.14\,mm^2$ for each bFGF condition (each $n = 6$), using $\times 200$ magnification.

2.6. Gene expression analysis

Quantitative real-time polymerase chain reaction (qRT–PCR) was performed to examine the changes in mRNA expression of ECM components and endogenous growth factors induced by exogenous bFGF. 1, 4, 7 and 14 days after seeding and treatment with bFGF, the samples were homogenized with a homogenizer (Asone Co., Tokyo, Japan) and total RNA was extracted from the cells in the CGS with Trizol reagent (Invitrogen), according to the manufacturer's protocol. The quantity and quality of the extracted RNA were evaluated by measuring the A260:280 ratio of each sample. Reactions were performed using GeneAmp polymerase chain reaction (PCR) system 9700 (Applied Biosystems, Foster City, CA, USA), using the following cycle parameters: 25 °C for 10 min, 37 °C for 120 min, 85 °C for 5 min and 4 °C for 5 min.

mRNA expression levels of endogenous fibroblast growth factor 2 (basic) (*Fgf2*), hepatocyte growth factor (*Hgf*), vascular endothelial growth factor type A (*Vegfa*), hyaluronan synthase 1 (*Has1*), *Has2* and *Has3*, procollagen types I (*Col1a1*) and III (*Col3a1*), matrix metalloproteinases (*Mmp1* and *Mmp8*) and fibronectin (*Fn*) were evaluated using the primer sequences listed in Table 1. Amplification was performed in a 20 µl reaction mixture containing 1 µl cDNA, 10 µl Power SYBR Green Master Mix (Applied Biosystems), 0.25 µM (final concentration) of each primer, and ribonuclease-free water under the following conditions: 95 °C for 10 min, 40 cycles of 95 °C for 15 s, and 60 °C for 1 min. Fluorescence was

Copyright © 2015 John Wiley & Sons, Ltd.

DOI: 10.1002/term

Table 1. Primer sequences

Gene	Forward primer	Reverse primer
Hyaluronic acid synthase 1	5′-TAGGTGCTGTTGGAGGAGATGTGA-3′	5′-AAGCTCGCTCCACATTGAAGGCTA-3′
Hyaluronic acid synthase 2	5′-ACTGGGCAGAAGCGTGGATTATGT-3′	5′-AACACCTCCAACCATCGGGTCTTCTT-3′
Hyaluronic acid synthase 3	5′-CCTCATCGCCACAGTCATACAA-3′	5′-CCACCAGCTGCACCGTTAGT-3′
Procollagen type I	5′-AGGCATAAAGGGTCATCGTGGCTT-3′	5′-AGTCCATCTTTGCCAGGAGAACCA-3′
Procollagen type III	5′-ATGAGCTTTGTGCAATGTGGGACC-3′	5′-ACTGACCAAGGTAGTTGCATCCCA-3′
Matrix metalloproteinase 1	5′-GGTGGCCAGAATAGCTGAATG-3′	5′-GCGTTTTGATATGCCC-3′
Matrix metalloproteinase 8	5′-CCATGGATCCAGGTTACCCCACT-3′	5′-TGTGGTCCACTGAAGAAGAGGAAGA-3′
Fibronectin	5′-AGATTCAGAGACCCGGACAT-3′	5′-AGTTGTGCCTGGGTAGGTCT-3′
Fibroblast growth factor 2	5′-AAGAACGGCGGCTTCTTCCT-3′	5′-CCCTTGATGGACACAACTCC-3′
Hepatocyte growth factor	5′-ACAAGGGCTTTCCATTCACT-3′	5′-CCAGTAGCATCGTTTTCTCG-3′
Vascular endothelial growth factor	5′-CGTCTACCAGCGCAGCTATTG-3′	5′-GTGAGGTTTGATCCGCATGAT-3′
β2-microglobulin	5′-TCACACTGAATTCACACCCACCGA-3′	5′-TGATTACATGTCTCGGTCCCAGGT-3′

detected with StepOne Plus (Applied Biosystems). The specificity of each primer was confirmed by a single-peak melting curve. Standard curves were used and the results are shown as the fold change relative to the baseline value (day 1, bFGF 0 ng/ml) of the target gene mRNA concentration normalized relative to mRNA levels of the housekeeping gene, *β2-microglobulin*. Each individual sample was tested in triplicate ($n = 6$).

2.7. ELISA

To ascertain the retention of bFGF binding to CGS, the quantitative measurement of bFGF on CGS was performed using the human FGF basic ELISA kit (R&D Systems, Minneapolis, MN, USA). The paracrine profile of bFGF from the cultivated sVF was also assessed, using the rat FGF basic ELISA kit (R&D Systems). After cultivation for 1, 4, 7 and 14 days at the concentration of bFGF 100 ng/ml, the samples were used for both assays. Scaffolds were extracted from the culture medium and dissolved with 1% collagenase B after rinsing with PBS three times to remove the culture medium totally. The solution was centrifuged and the supernatants were collected to measure the concentrations of bFGF according to the manufacturer's instructions, then the total quantity of binding bFGF on CGS was calculated. The secreted bFGF from the cultivated cells was investigated by measuring the rat-derived bFGF concentrations in the culture medium. Each individual sample was tested in triplicate ($n = 6$). Data were normalized by cell numbers.

2.8. Surgical procedure and implantation of collagen–gelatin sponge

The surgical procedures that were used for generating vocal fold injuries were established in previous studies (Hirano *et al*., 2004; Ohno *et al*., 2011). All beagles were sedated under general anaesthesia with an intramuscular injection of ketamine hydrochloride (15 mg/kg) and xylazine hydrochloride (6 mg/kg). The larynx was visualized using a direct laryngoscope and the right vocal folds were unilaterally scarred by stripping the entire layer of the lamina propria down to the muscle with microscissors and microforceps. The contralateral vocal folds were left intact as normal controls. Six weeks after the initial surgery, the animals were sedated again and implantation of CGS was performed, using a direct laryngoscope as described above.

Before implantation, $5 \times 2\,mm^2$ and 3 mm thick CGS were prepared and impregnated with 10 μl normal saline solution (Otsuka Pharmaceutical, Tokyo, Japan) or 10 μl bFGF solution (7 $\mu g/cm^2$) and incubated overnight at 4 °C. A vertical incision along the longitudinal axis of the vocal fold was made on the superior lateral surface of the vocal fold, using microscissors, and the epithelium was gently lifted to form a pocket in the subepithelial layer, into which a CGS could be placed. The beagles underwent implantation of a CGS impregnated with saline only (CGS group; $n = 5$) or a CGS with bFGF (CGS + bFGF group; $n = 5$) into the subepithelial pocket of one vocal fold. The animals that had nothing implanted were the sham-treated group ($n = 5$). The wounds were covered by fibrin glue (Bolheal; Kaketsuken, Kumamoto, Japan) to prevent loss or dislocation of the implanted material (Figure 1). The dose of

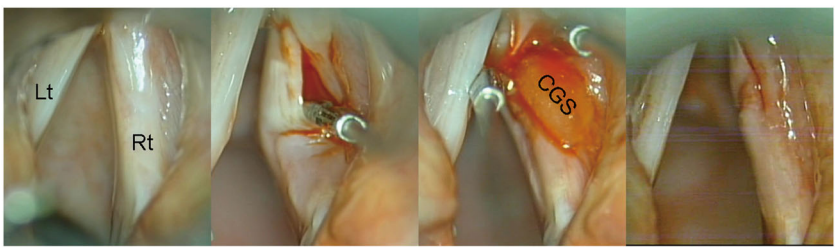

Figure 1. Surgical procedure: right side, scarred vocal fold; CGS was implanted in a subepithelial space after lifting the epithelium; Rt, right vocal fold; Lt, left vocal fold; CGS, collage–gelatin sponge

Copyright © 2015 John Wiley & Sons, Ltd.

DOI: 10.1002/term

7 μg/cm^2 bFGF was determined based on previous reports that had demonstrated significantly superior wound closure or neoformed capillaries at the injured skin or palatine membrane with the combination of CGS and 7 μg/cm^2 bFGF, as opposed to other bFGF concentrations (Kanda *et al*., 2012). All surgical procedures for stripping and implantation were conducted by one professional laryngologist (S.H.).

All animals were euthanized 5 months after the surgery by intracardiac injection of pentobarbital. The larynges were harvested and used for vibratory examinations and then subjected to histological examination.

2.9. Vibratory examination of excised larynges

Vocal fold vibrations were examined using an excised larynx set-up, as described in previous studies (Kishimoto *et al*., 2010; Ohno *et al*., 2011). For better visualization of the vocal fold, supraglottic structures such as the epiglottis, false vocal folds and aryepiglottic folds were removed after resection of the superior portion of the thyroid cartilage. The arytenoid cartilages were sutured together, and an arytenoid adduction procedure was performed bilaterally, using 3-0 Prolene to close the glottis. After the larynx had been mounted on a table, an endotracheal tube was inserted and tightly clamped to prevent air leaks. Air was pumped through the tube to generate vocal fold vibrations. The larynges were irrigated with saline throughout the experiment to keep the vocal folds moist. To record fine details of the vocal fold vibrations, a high-speed digital imaging system (Memrecam Ci; NAC Image Technology, Osaka, Japan) was mounted 50 cm above the larynx and the images were recorded at a frame rate of 4000 frames/s.

In this experiment, we adopted three objective parameters or measurements for functional examination: (a) phonation threshold pressure (*PTP*); (b) normalized mucosal wave amplitude (*NMWA*); and (c) normalized glottal gap (*NGG*). *PTP* is defined as the minimum amount of subglottal pressure required to initiate vocal fold oscillation, and regulated by factors such as vocal fold thickness, stiffness and glottal width (Titze, 1988, 1992). The amplitude of the mucosal wave was measured to evaluate the mucosal vibration and elasticity of the vocal fold structures, especially the lamina propria, using ImageJ software (National Institutes of Health, Bethesda, MD, USA). The distance ($d1$) from the midline of the glottis to the free edge of the vocal fold was measured at the anteroposterior middle portion of the vocal fold during the closed phase; the closed phase was determined based on the motion of the upper and lower lips of the vocal folds. The same distance ($d2$) was measured at the maximum open phase. The mucosal wave amplitude was defined by subtracting $d1$ from $d2$ and was normalized by dividing the subtracted digit by the anteroposterior length of the glottis (L), which was measured from the anterior commissure to the vocal process. The following formula was used:

$$NMWA = (d2–d1)/L \times 100\,\text{units}\,(\text{U})$$

The normalized glottal gap (*NGG*) was calculated to evaluate glottis closure during the closed phase. The glottal gap area (a) was measured using ImageJ software and normalized by dividing this value by L^2. The following formula was used:

$$NGG = a/L2 \times 100\,(\text{U}).$$

All procedures from extraction of the larynx to the vibratory examination were performed in a same operation room under same temperature (24 °C) and the vibratory examination was completed in 10 min for each sample.

2.10. Histological examination

Histological analyses were completed to evaluate changes in the ECM or the degree of scar contraction of the scarred vocal folds. Immediately after the vibratory examination, the larynges were fixed in 10% formaldehyde for tissue examination. The larynges were subsequently embedded in paraffin and 5 μm thick serial sections were prepared in the coronal plane from the anteroposterior middle portion of the vocal folds. Elastica van Gieson staining was performed to identify collagen and elastin; Alcian blue staining and a hyaluronidase digestion technique were performed to identify HA. Images were captured with a Biorevo BZ-9000 microscope (Keyence, Osaka, Japan).

The sections were examined at × 4– × 40 magnification. The areas of stained HA, dense collagen deposition and elastin of the LP were measured using software that automatically measures an area with a designated colour threshold (Biorevo BZ-H1C and BZ-H1M; Keyence). To evaluate the density of the HA, collagen or elastin area in each LP, we totalled the areas stained for HA, collagen or elastin in the injured vocal folds and they were divided by the total LP areas. The amount of HA in the LP was determined by subtracting the ratio of the blue-stained area of the section with hyaluronidase digestion from that of an adjacent section without digestion.

The thickness of the LP was also assessed to determine the degree of scar contraction. The LP thickness was determined by measuring the distance from the free edge of the vocal fold down to the thyroarytenoid muscle, and normalized by dividing the distance on the treated side ($t1$) by that of the normal side ($t2$). The following formula was used:

$$\text{normalized thickness of lamina propria}\,(NTLP) = t1/t2.$$

These assessments were performed in a blinded fashion, in which the examiners were not informed of the group to which each slide belonged.

2.11. Statistical analysis

Two-way factorial analysis of variance (ANOVA), followed by a Tukey–Kramer *post hoc* test, was performed to

Copyright © 2015 John Wiley & Sons, Ltd.

DOI: 10.1002/term

compare cell proliferation and gene expression for each bFGF condition, to investigate any statistical differences between the conditions at each time point. When interactions were present between the concentration and experimental time point, one-way factorial ANOVA followed by a Tukey–Kramer *post hoc* test was performed. For comparisons of the *in vitro* apoptosis assay and dedifferentiation assay, and all *in vivo* experiments, one-way factorial ANOVA followed by a Tukey–Kramer *post hoc* test was performed. Statistical significance was defined as $p < 0.01$ or $p < 0.05$, using StatView 5.0 (SAS Institute, Berkeley, CA, USA). All data are expressed as mean ± standard deviation (SD).

3. Results

3.1. Quantification of cell proliferation

To assess cell growth in CGS, sVF proliferation was quantified over a 14 day period. Between days 7 and 14, the number of cells cultured with 100 ng/ml bFGF was significantly higher than the number of cells cultured with 0 or 1 ng/ml bFGF (all $p < 0.01$, except for day 10 vs 1 ng/ml; $p < 0.05$). Cells cultured with 10 ng/ml bFGF also showed a significantly higher amount of growth at day 14 compared with the 0 ng/ml bFGF condition (Figure 2).

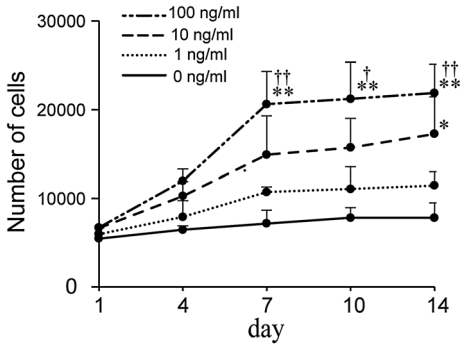

Figure 2. Proliferation time course of scar fibroblasts; data are presented as mean ± SD of assays run in triplicate ($n = 6$); $^{**}p < 0.01$, $^{*}p < 0.05$ compared with 0 ng/ml bFGF; $^{\dagger\dagger}p < 0.01$, $^{\dagger}p < 0.05$ compared with 1 ng/ml bFGF

3.2. Effect of bFGF on CC3 and αSMA expression

To investigate whether bFGF had a concentration-dependent effect on sVF apoptosis,, immunohistochemistry for CC3 staining was performed (Figure 3A). The number of cells that were double-positive for CC3 and GFP in the 100 ng/ml bFGF group was significantly decreased compared with the 0 ng/ml group ($p < 0.05$) (Figure 3B). We also investigated αSMA expression, which indicates the existence of myofibroblasts. The number of double-positive cells for αSMA and GFP appeared to decrease in a dose-dependent manner (Figure 3A), and the ratio of positive cells was significantly lower at the 100 ng/ml bFGF concentration compared to 0 and 10 ng/ml ($p < 0.01$). The 10 ng/ml bFGF group also showed

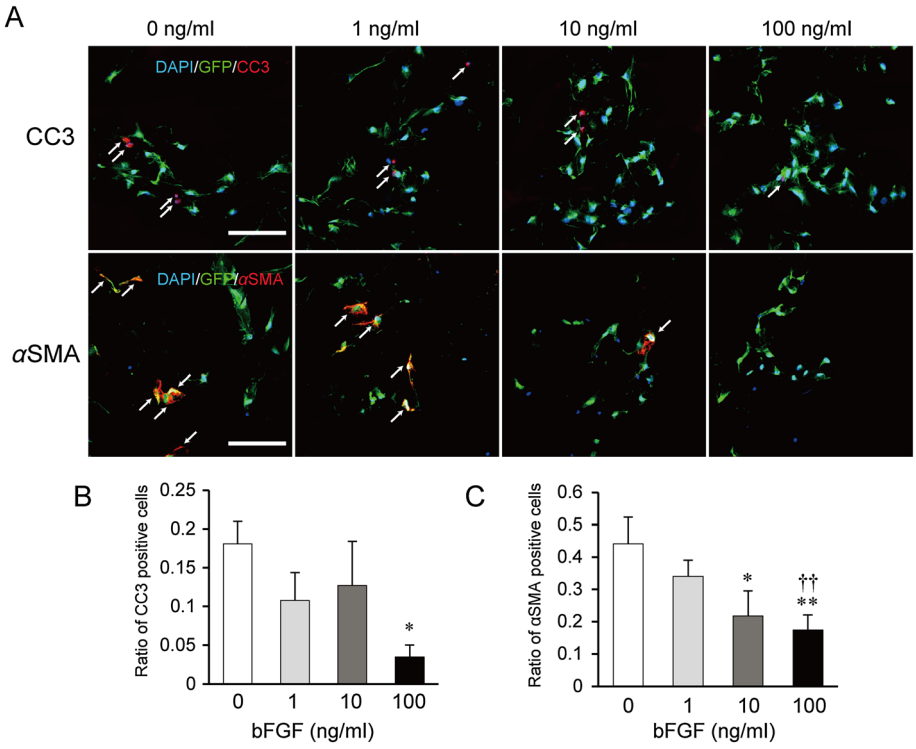

Figure 3. Representative confocal images showing immunohistochemical analysis on day 7 after bFGF administration. (A) Blue, DAPI; green, GFP; red, CC3 or αSMA; double positive for GFP and CC3 or GFP and αSMA indicate apoptotic cells and myofibroblasts, respectively (white arrow); scale bars = 100 μm. (B) Ratio of CC3-positive cells was calculated from six samples in each bFGF group; $^{*}p < 0.05$ compared with 0 ng/ml bFGF. (C) Ratio of αSMA-positive cells was calculated from six samples in each bFGF group; $^{**}p < 0.01$, $^{*}p < 0.05$ compared with 0 ng/ml bFGF; $^{\dagger\dagger}p < 0.01$ compared with 1 ng/ml bFGF; data are presented as mean ± SD

Copyright © 2015 John Wiley & Sons, Ltd.

DOI: 10.1002/term

significant suppression of αSMA compared with the 0 ng/ml group ($p < 0.05$) (Figure 3C).

3.3. Effects of bFGF on ECM gene expression

To determine the efficacy of bFGF administration, the mRNA expression levels of endogenous growth factors (*Fgf2*, *Hgf* and *Vegfa*) and ECM components (*Has 1*, *Has 2*, *Has 3*, *Col1a1*, *Col3a1*, *Mmp1*, *Mmp8* and *Fn*) were measured by RT–PCR. *Has 1* and *Has 3* showed a similar dose-dependent pattern from day 4 and significantly higher levels at the 100 ng/ml bFGF concentration. Meanwhile, *Has 2* was expressed to significantly higher levels in the bFGF 10 ng/ml group until day 4 (Figure 4A–C). The expression levels of *Col1a1* were significantly lower in the presence of 10 and 100 ng/ml bFGF than with 1 ng/ml on day 4, as well as with 0 and 1 ng/ml on day 7. *Col3a1* showed a similar suppression pattern in the 10 and 100 ng/ml groups compared to the 0 or 1 ng/ml groups until day 4, whereas from day 7, for all bFGF conditions, significant suppression was observed compared to the 0 ng/ml group. A noticeable upregulation of *Mmp1* and *Mmp8* expression emerged on day 14, although all levels showed wide variations (Figure 4D–G).

The expression levels of endogenous growth factors showed significant upregulation in the 100 ng/ml bFGF group as early as day 1 and the levels tapered after reaching the maximum levels on day 4. The upregulation of *Hgf* expression showed a slightly slow start compared to *Fgf2* or *Vegfa*, but reached markedly high levels with 100 ng/ml bFGF (Figure 4I–K).

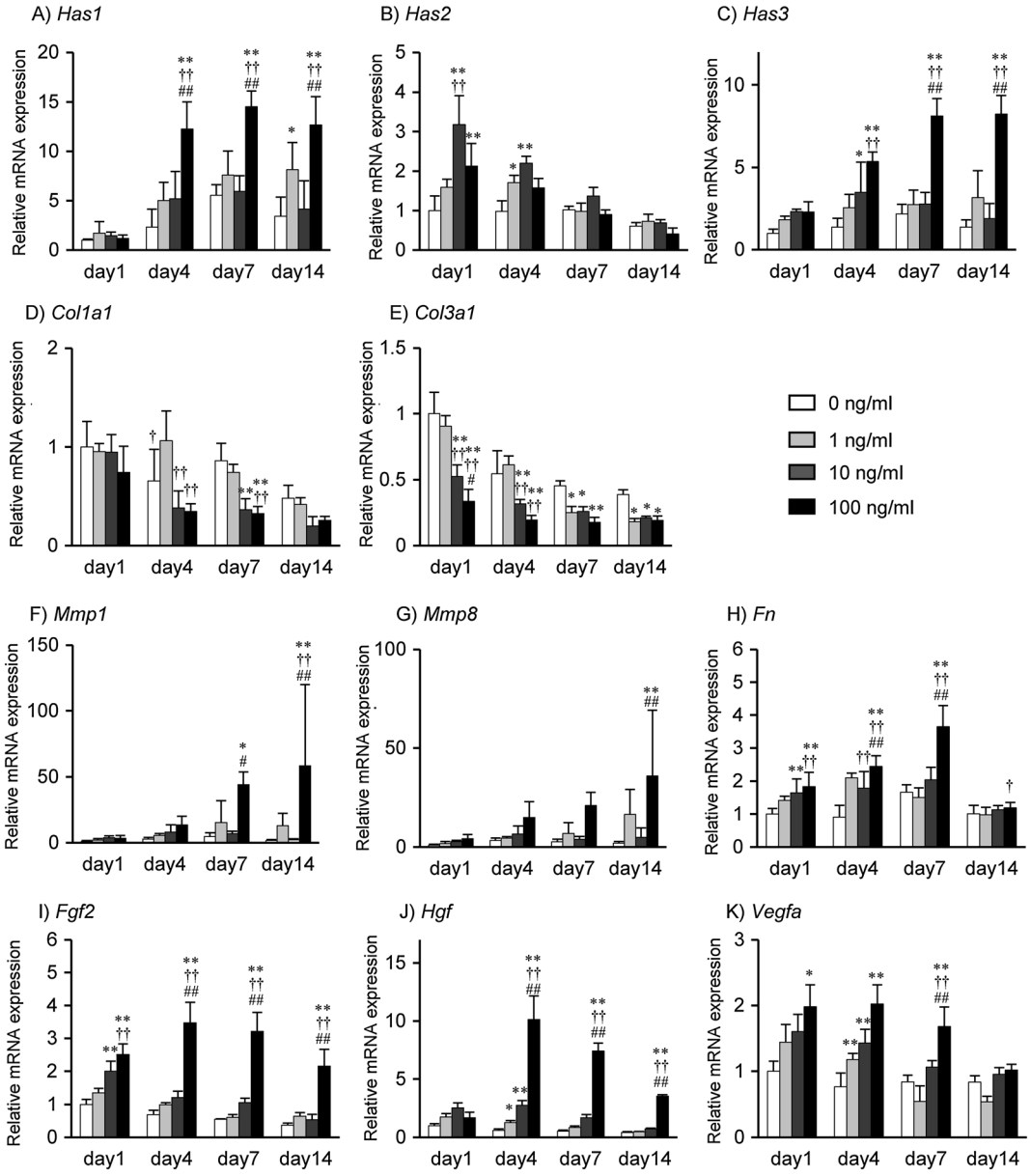

Figure 4. Gene expression (mRNA) ratios of scar fibroblasts, normalized relative to the housekeeping gene β2-microglobulin: the expression level with 0 ng/ml bFGF on day 1 was used as the baseline value and defined as 1.0; data are presented as mean ± SD of assays run in triplicate ($n = 6$); $^{*}p < 0.05$, $^{**}p < 0.01$ compared with 0 ng/ml bFGF; $^{\dagger\dagger}p < 0.01$, $^{\dagger}p < 0.05$ compared with 1 ng/ml bFGF; and $^{\#\#}p < 0.01$, $^{\#}p < 0.05$ compared with 10 ng/ml bFGF

Copyright © 2015 John Wiley & Sons, Ltd.

DOI: 10.1002/term

3.4. Retention of exogenous bFGF and the production of endogenous bFGF

Analysis of the quantity of initially loaded human bFGF revealed that CGS bound and immobilized bFGF through 14 days, gradually releasing the initially binding bFGF (see supporting information, Table S1). The paracrine secretion of bFGF from sVFs was gradually decreasing but sustained release under the condition of bFGF 100 ng/ml (see supporting information, Table S2).

3.5. Vibratory examination of excised larynges

Digital high-speed images revealed a limited mucosal wave of the injured vocal fold (right side) compared to the contralateral intact (left) side and a severe glottal gap in the sham-treated group (Figure 5A). The CGS + bFGF group showed better vibration in the injured side and the glottal gap had almost disappeared in the closed phase (Figure 5C), while the CGS group retained limited vibration, even though this group achieved a reduction in the glottis gap (Figure 5B).

The CGS + bFGF group showed significantly lower *PTP* compared to the sham-treated group ($p < 0.05$) (Figure 6A) and a higher ratio of *NMWA* compared to the CGS group and the sham-treated group ($p < 0.05$) (Figure 6B). Both the CGS and CGS + bFGF groups showed significantly smaller *NGG* than the sham-treated group (CGS group, $p < 0.05$; CGS + bFGF group, $p < 0.01$). No significant differences were observed in the *PTP* and *NGG* parameters between the CGS and CGS + bFGF groups.

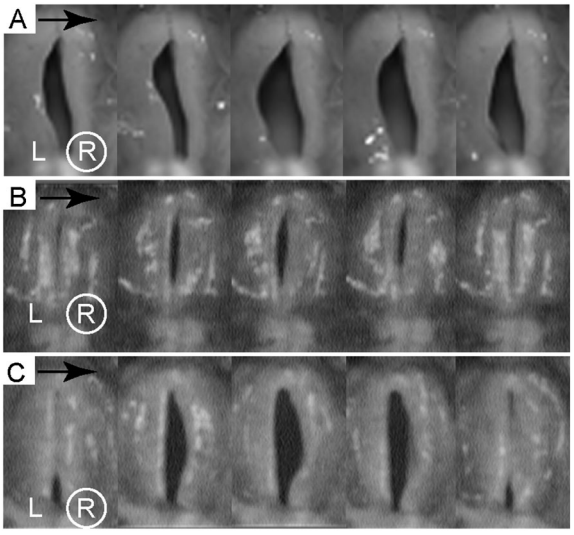

Figure 5. Representative digital high-speed images of vocal fold vibratory patterns: (A) sham-treated group; (B) CGS group; (C) CGS + bFGF group; smaller glottal gaps were observed in both the CGS and CGS + bFGF groups during the closed phase; better mucosal waves in treated vocal folds in the CGS + bFGF group were observed, while vibrations in the CGS group were limited; L, left vocal fold (intact side); R, right vocal fold (injured and treated side)

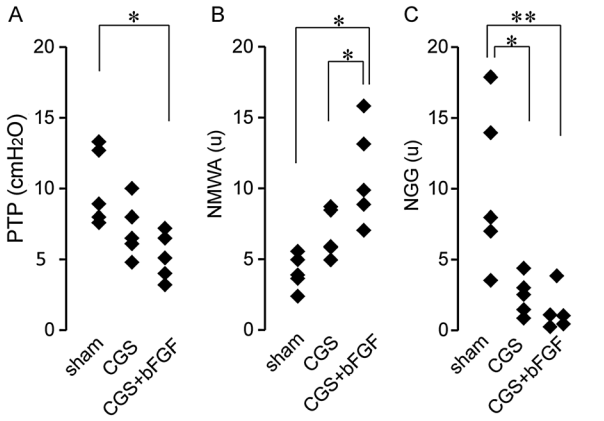

Figure 6. Results of vibratory examinations; data for all beagles in each group are plotted (each $n = 5$): (A) phonation threshold pressure (PTP); (B) normalized mucosal wave amplitude (NMWA); (C) normalized glottal gap (NGG); $^{**}p < 0.01$, $^{*}p < 0.05$

3.6. Histological examination

Alcian blue staining revealed better restoration in the CGS + bFGF-treated vocal folds compared to the sham-treated group (Figure 7A). The density of HA in the CGS + bFGF group was significantly greater than in the sham-treated group ($p < 0.01$) and the CGS group ($p < 0.05$) (Figure 7B). Elastica van Gieson staining revealed the suppression of dense collagen deposition and reorganization of elastin in the injured vocal folds of the CGS and CGS + bFGF groups compared to the sham-treated group (Figure 7A). The densities of collagen deposition were significantly lower in the two implantation groups compared to the sham-treated group ($p < 0.01$), while this suppression was significantly greater in the CGS + bFGF group compared to the CGS group ($p < 0.01$) (Figure 7C). The densities of elastin were also significantly higher only in the CGS + bFGF group than the sham-treated group ($p < 0.01$) (Figure 7D). *NTLP* was higher in both of the implanted vocal folds relative to the sham-treated group (CGS, $p < 0.05$; CGS + bFGF, $p < 0.01$) but no significant differences were observed between the two implanted groups (Figure 7E). No residual CGS was found in any specimen.

4. Discussion

Vocal fold scar continues to present a therapeutic challenge. Various surgical injections or implantation therapies have been tried, including fat implants (Sataloff *et al*., 1997), collagen injection (Remacle *et al*., 2000) and fascia implants (Tsunoda *et al*., 1999), with each approach showing certain capacities to alleviate issues such as glottal incompetence. However, these effects were shown to be temporary. The main obstacle to effective vocal fold scar treatment lies in the difficulty of addressing disorganized ECM components, such as lost HA or

Copyright © 2015 John Wiley & Sons, Ltd.

DOI: 10.1002/term

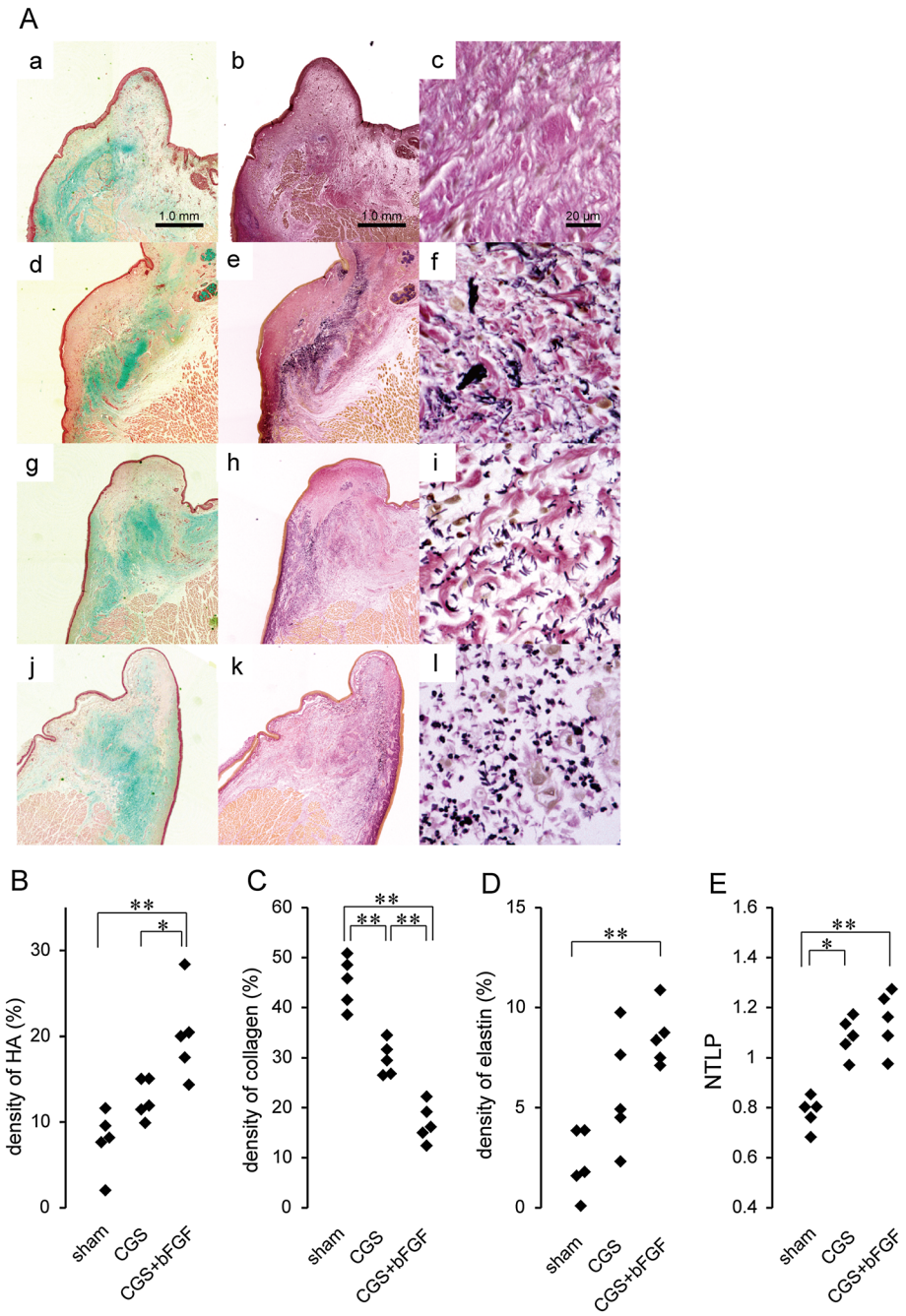

Figure 7. **(A) Representative images of histological examinations: Alcian blue staining (a, d, g, j) and elastica van Gieson staining (b, e, h, k, ×4 magnification; c, f, i, l, ×40 magnification) of the sham-treated group (a–c), the CGS group (d–f), the CGS + bFGF group (g–i) and the normal vocal fold (j–l); the CGS + bFGF group showed better hyaluronic acid restoration (blue-stained area); tissue contraction and dense collagen deposition was reduced and reorganization of elastin were observed in both implanted groups. (B–E) Data for histological examination from all beagles in each group are plotted (each $n = 5$): (B) density of hyaluronic acid; (C) density of dense collagen deposition; (D) density of elastin; (E) normalized thickness of the lamina propria (NTLP); $^{**}p < 0.01$, $^{*}p < 0.05$**

excessive collagen accumulation. A combination therapy of CGS and bFGF could be undertaken as a tissue-engineering concept because other than scaffold (CGS) and growth factor (bFGF), cells encountering around CGS or infiltrating into CGS are involved. In the current study, we evaluated the therapeutic efficacy of the combination of CGS and bFGF to treat vocal fold scar in beagle models, and analysed the potential mechanisms of its restorative effects using rat sVFs.

4.1. *In vitro* findings

Previously, we assessed the biocompatibility of CGS for non-scarred, normal vocal fold fibroblasts cultivated in a three-dimensional (3D) manner for short periods of time (Hiwatashi *et al.*, 2014). In this study, we used longer time points in order to integrate the results *in vivo*, because Takemoto *et al.* (2008) reported that around 60% of impregnated bFGF remained in the CGS 7 days after

Copyright © 2015 John Wiley & Sons, Ltd.

DOI: 10.1002/term

implantation in the backs of mice, with 30% remaining on post-implantation day 10.

We observed significantly lower numbers of apoptotic cells with bFGF at 100 ng/ml, and dose-dependent decreases in the number of αSMA-expressing cells, myofibroblasts. Previous studies revealed that bFGF has the potential to protect many types of cells against apoptosis, and that bFGF is a possible inducer of apoptosis in myofibroblasts during scar formation (Funato *et al*., 1997; Shi *et al*., 2013). bFGF was also reported to prevent fibroblasts in scar tissue from changing their phenotype into myofibroblasts (Spyrou and Naylor, 2002). In the context of these reports and our results at day 7 of sVF cultivation, it is possible that bFGF promoted the apoptosis of myofibroblasts, while bFGF accelerated the growth of fibroblasts, leading to the dominance of the fibroblasts and a reduction of the apoptotic cells in a dose-dependent manner. This assumption is in agreement with our results for the cell proliferation assay that showed a growth spurt after day 4. However, there is a limitation in these assays, in that we did not separate the fibroblasts and myofibroblasts and did not conduct discrete experiments to compare their cell behaviour. Nonetheless, the use of excised injured vocal fold tissue is preferable, because these cells likely more accurately reflect the biological reactions to bFGF *in vivo*. In each condition, cell growth persisted for 7 days, followed by linear growth after day 7. Earlier studies investigating the proliferation of vocal fold fibroblasts in 3D scaffolds only demonstrated two phases of growth until day 7, lag and log (Chen and Thibeault, 2010). Grayson *et al*. (2004) displayed the two phases followed by a plateau phase with longer cell cultivation in 3D, and concluded that the ECM network produced by the cells influenced the cell proliferation potential. Among various ECM components, fibronectin contributes to cell–matrix adhesion of fibroblasts and the gene expression of *fn* showed that the highest level on day 7, followed by downregulation until day 14, may support the transition of cell growth in this study.

Has 1 and *Has 3* gene expression showed upregulation from day 4 that persisted until day 14 with 10 ng/ml and 100 ng/ml bFGF. *Has* is a progenitor of HA, which is thought to be a key molecule in maintaining the viscoelasticity of vocal folds (Gray *et al*., 1999), and reduction of HA levels in human vocal folds has been correlated with changes in their viscoelastic properties (Chan et al., 2001). Our finding that *Has* is upregulated in response to bFGF treatment could suggest that sVFs infiltrating into the CGS reorganize and restore greater amounts of HA following bFGF stimulation *in vivo*. Exogenous bFGF down-regulated the expression of *Col1a1* and *Col3a1* during days 4–7 and these significant changes were retained until day 14. These two genes are related to type I and type III collagen, respectively. Type III collagen is rapidly synthesized as a wound matrix and is in turn gradually replaced by type I collagen. Excessive deposition of type I collagen is a main feature of scar tissue, because it provides long-term tensile strength and increases stiffness (Stephens and Thomas, 2002). MMP induces ECM turnover through the degradation and production of collagen, and our results showed that *Mmp1* and *Mmp8* were indeed upregulated in the presence of 100 ng/ml bFGF. Taken together, infiltrating sVFs into the CGS may suppress excessive collagen production and alleviate collagen deposition.

With regard to endogenous growth factors, all examined growth factors showed significant upregulation in the bFGF 100 ng/ml group, especially for *Fgf2* and *Hgf*, which showed markedly increases from day 4 that continued until day 14. HGF has a strong anti-fibrotic effect that is attributed to the resolution of fibrosis. In canine vocal scar models, HGF administration was revealed to have potential for restoring HA and decreasing collagen deposition (Hirano *et al*., 2003). Our results showing an upregulation of *Fgf2* suggest that exogenous bFGF stimulates the sVF in the CGS and increases endogenous bFGF. Moreover, this autocrine bFGF loop may not only stimulate HGF production, resulting in a better antifibrotic effect, but could also strengthen HA production and enhance the suppression of excessive collagen.

4.2. *In vivo* findings

Scaffolds should provide a space that is suitable for the induction of tissue regeneration in which self-derived cells surrounding the scaffold, or preseeded cells, infiltrate the scaffold and proliferate (Tabata *et al*., 1999). In our study, the *NTLP* of the two CGS implanted groups was significantly larger than in the sham-treated group, and a reduced *NGG* was subsequently shown for both groups. As the preferable collagen sponge pore size for adhesive interaction of fibroblasts is considered to be 50–200 μm (Geiger *et al*., 2009), the length of CGS pore used here, which was > 80 μm (Takemoto *et al*., 2008), is compatible. Based on previous reports using collagen sponges (Suzuki *et al*., 1990), within 2 or 3 weeks the CGS would likely also be biodegraded and replaced by a natural ECM that is produced by the cells recruited into the scaffold. Considering the CGS biomaterial features, our results indicate that sVFs around the CGS infiltrated into the CGS, whereupon the CGS was degraded and replaced by the regenerated tissue during the wound-healing process. A functional examination revealed significant amelioration of the *NMWA* in the CGS + bFGF group compared to the CGS implanted group. This result could be due to differences in ECM reorganization, including significant improvement of HA and reduction of collagen. As mentioned above, HA is indispensable for retaining the viscoelasticity of vocal folds, while excessive collagen accumulation stiffens vocal folds. Thus, it is possible that sustained release of bFGF stimulated the sVF to colonize in and around the CGS to promote the restoration of typical ECM distributions.

In the current study, we set only the CGS group as controls *in vivo*, and another control treated by bFGF only was not prepared, because administration of bFGF only is usually performed by injection, and the procedure is quite

Copyright © 2015 John Wiley & Sons, Ltd.

DOI: 10.1002/term

different from the current implant operation of CGS. The wound-healing process should be different, because of different tissue damage caused by each procedure. Instead, our group has previously obtained functional and histological data of beagles treated with bFGF injection therapy under the same setting as the current study (Suehiro *et al*., 2010), and the comparative analysis with the current data was completed (see supporting information, Figures S1, S2). Although this is not a rigid comparison, the data show that the combination therapy of CGS and bFGF is superior to the bFGF injection therapy in both the functional and histological examinations.

Taking the *in vitro* and *in vivo* results together, the current study demonstrates that the combination therapy of CGS and bFGF shows better efficacy for vocal fold scar in terms of histological and functional regeneration compared to the group with CGS implanted alone or the sham-treated group. The mechanisms of the favourable effects are thought to be derived from the sustained release system of bFGF, which activates sVF to control ECM redistribution. However, there may be a limitation, that the extent of improvement varies among individuals, and extended observation may be needed to evaluate the therapeutic endpoint.

5. Conclusions

The current study demonstrated that the combination therapy of CGS and bFGF has significant potential to improve vibratory properties and promote histological changes, including better restoration of HA and elastin, with reduced collagen deposition and tissue contraction. Sustained release of bFGF regulates ECM synthesis, leading to ECM redistribution. Together, these results suggest that CGS with bFGF may have therapeutic efficacy for the treatment of vocal fold scar.

Conflict of interest

The authors have declared that there is no conflict of interest.

Acknowledgements

We acknowledge Tsuguyoshi Taira from Gunze Research and Development Centre for CGS preparation. This study was supported by the Advanced Research for Medical Products Mining Programme of the National Institute of Biomedical Innovation and the Ministry of Health and Welfare, Japan.

References

Ayvazyan A, Morimoto N, Kanda N *et al.* 2011; Collagen–gelatin scaffold impregnated with bFGF accelerates palatal wound healing of palatal mucosa in dogs. *J Surg Res* **171**: e247–257.

Chan RW, Gray SD, Titze IR 2001; The importance of hyaluronic acid in vocal fold biomechanics. *Otolaryngol Head Neck Surg* **124**: 607–614.

Chen X, Thibeault SL 2010; Biocompatibility of a synthetic extracellular matrix on immortalized vocal fold fibroblasts in 3D culture. *Acta Biomater* **6**: 2940–2948.

Desmouliere A 1995; Factors influencing myofibroblast differentiation during wound healing and fibrosis. *Cell Biol Int* **19**: 471–476.

Funato N, Moriyama K, Shimokawa H *et al.* 1997; Basic fibroblast growth factor induces apoptosis in myofibroblastic cells isolated from rat palatal mucosa. *Biochem Biophys Res Commun* **240**: 21–26.

Geiger B, Spatz JP, Bershadsky AD 2009; Environmental sensing through focal adhesions. *Nat Rev Mol Cell Biol* **10**: 21–33.

Gospodarowicz D 1974; Localisation of a fibroblast growth factor and its effect alone and with hydrocortisone on 3 T3 cell growth. *Nature* **249**: 123–127.

Gray SD, Titze IR, Chan R *et al.* 1999; Vocal fold proteoglycans and their influence on biomechanics. *Laryngoscope* **109**: 845–854.

Grayson WL, Ma T, Bunnell B 2004; Human mesenchymal stem cells tissue development in 3D PET matrices. *Biotechnol Prog* **20**: 905–912.

Hirano M 1974; Morphological structure of the vocal cord as a vibrator and its variations. *Folia Phoniatr (Basel)* **26**: 89–94.

Hirano S 2005; Current treatment of vocal fold scarring. *Curr Opin Otolaryngol Head Neck Surg* **13**: 143–147.

Hirano S, Bless D, Heisey D, *et al.* 2003; Roles of hepatocyte growth factor and transforming growth factor-β1 in production of extracellular matrix by canine vocal fold fibroblasts. *Laryngoscope* **113**: 144–148.

Hirano S, Bless DM, Nagai H *et al.* 2004; Growth factor therapy for vocal fold scarring in a canine model. *Ann Otol Rhinol Laryngol* **113**: 777–785.

Hirano S, Minamiguchi S, Yamashita M *et al.* 2009; Histologic characterization of human scarred vocal folds. *J Voice* **23**: 399–407.

Hiwatashi N, Hirano S, Mizuta M *et al.* 2014; Biocompatibility and efficacy of collagen/gelatin sponge scaffold with sustained release of basic fibroblast growth factor on vocal fold fibroblasts in three-dimensional culture. *Ann Otol Rhinol Laryngol* **124**: 116–125.

Isogai N, Morotomi T, Hayakawa S *et al.* 2005; Combined chondrocyte–copolymer implantation with slow release of basic fibroblast growth factor for tissue engineering an auricular cartilage construct. *J Biomed Mater Res A* **74**: 408–418.

Ito T, Suzuki A, Imai E *et al.* 2001; Bone marrow is a reservoir of repopulating mesangial cells during glomerular remodeling. *J Am Soc Nephrol* **12**: 2625–2635.

Jette ME, Hayer SD, Thibeault SL 2013; Characterization of human vocal fold fibroblasts derived from chronic scar. *Laryngoscope* **123**: 738–745.

Kanda N, Morimoto N, Takemoto S *et al.* 2012; Efficacy of novel collagen/gelatin scaffold with sustained release of basic fibroblast growth factor for dermis-like tissue regeneration. *Ann Plast Surg* **69**: 569–574.

Kishimoto Y, Hirano S, Kitani Y, *et al.* 2010; Chronic vocal fold scar restoration with hepatocyte growth factor hydrogel. *Laryngoscope* **120**: 108–113.

McGee GS, Davidson JM, Buckley A *et al.* 1988; Recombinant basic fibroblast growth factor accelerates wound healing. *J Surg Res* **45**: 145–153.

Morimoto N, Yoshimura K, Niimi M *et al.* 2013; Novel collagen/gelatin scaffold with sustained release of basic fibroblast growth factor: clinical trial for chronic skin ulcers. *Tissue Eng A* **19**: 1931–1940.

Ohno S, Hirano S, Kanemaru S *et al.* 2011; Implantation of an atelocollagen sponge with autologous bone marrow-derived mesenchymal stromal cells for treatment of vocal fold scarring in a canine model. *Ann Otol Rhinol Laryngol* **120**: 401–408.

Remacle M, Lawson G, Degols JC *et al.* 2000; Microsurgery of sulcus vergeture with carbon dioxide laser and injectable collagen. *Ann Otol Rhinol Laryngol* **109**: 141–148.

Rousseau B, Hirano S, Chan RW *et al.* 2004; Characterization of chronic vocal fold scarring in a rabbit model. *J Voice* **18**: 116–124.

Rousseau B, Hirano S, Scheidt TD, *et al.* 2003; Characterization of vocal fold scarring in a canine model. *Laryngoscope* **113**: 620–627.

Sataloff RT, Spiegel JR, Hawkshaw M *et al.* 1997; Autologous fat implantation for vocal fold scar: a preliminary report. *J Voice* **11**: 238–246.

Shi HX, Lin C, Lin BB *et al.* 2013; The anti-scar effects of basic fibroblast growth

Copyright © 2015 John Wiley & Sons, Ltd.

DOI: 10.1002/term

factor on the wound repair *in vitro* and *in vivo*. *PLoS One* **8**: e59966.
Spyrou GE, Naylor IL 2002; The effect of basic fibroblast growth factor on scarring. *Br J Plast Surg* **55**: 275–282.
Stephens P, Thomas DW 2002; The cellular proliferative phase of the wound repair process. *J Wound Care* **11**: 253–261.
Suehiro A, Hirano S, Kishimoto Y *et al.* 2010; Treatment of acute vocal fold scar with local injection of basic fibroblast growth factor: a canine study. *Acta Otolaryngol* **130**: 844–850.
Suzuki S, Matsuda K, Isshiki N *et al.* 1990; Experimental study of a newly developed bilayer artificial skin. *Biomaterials* **11**: 356–360.
Tabata Y, Nagano A, Ikada Y 1999; Biodegradation of hydrogel carrier incorporating fibroblast growth factor. *Tissue Eng* **5**: 127–138.
Takemoto S, Morimoto N, Kimura Y *et al.* 2008; Preparation of collagen/gelatin sponge scaffold for sustained release of bFGF. *Tissue Eng A* **14**: 1629–1638.
Tateya T, Tateya I, Sohn JH *et al.* 2005; Histologic characterization of rat vocal fold scarring. *Ann Otol Rhinol Laryngol* **114**: 183–191.
Thibeault SL, Li W, Bartley S 2008; A method for identification of vocal fold lamina propria fibroblasts in culture. *Otolaryngol Head Neck Surg* **139**: 816–822.
Titze IR 1988; The physics of small-amplitude oscillation of the vocal folds. *J Acoust Soc Am* **83**: 1536–1552.
Titze IR 1992; Phonation threshold pressure: a missing link in glottal aerodynamics. *J Acoust Soc Am* **91**: 2926–2935.
Tsunoda K, Takanosawa M, Niimi S 1999; Autologous transplantation of fascia into the vocal fold: a new phonosurgical technique for glottal incompetence. *Laryngoscope* **109**: 504–508.

Supporting information

The following supporting information may be found in the online version of this article:

Figure S1. Results of vibratory examinations
Figure S2. Results of histological examinations
Table S1. Time course of bFGF retention on collagen-gelatin sponge
Table S2. Time course of endogenous bFGF levels

Copyright © 2015 John Wiley & Sons, Ltd.

DOI: 10.1002/term

Supporting information

TABLE 2 Supporting Information

TABLE 2 : Retention of bFGF on collagen/gelatin sponge

Total quantity of binding bFGF (pg) (mean ± SD)							
Day 1		Day 4		Day 7		Day 14	
315.2	62.1	135.3	9.8	44.6	6.3	20	1.7

TABLE 3 Supporting Information

TABLE 3 : Endogenous bFGF upon addition of exogenous human bFGF

bFGF levels (pg/mL) (mean ± SD)							
Day 1		Day 4		Day 7		Day 14	
48.2	10.5	42.6	8.6	27	2.7	23.1	3.6

Figure 8 Supporting information

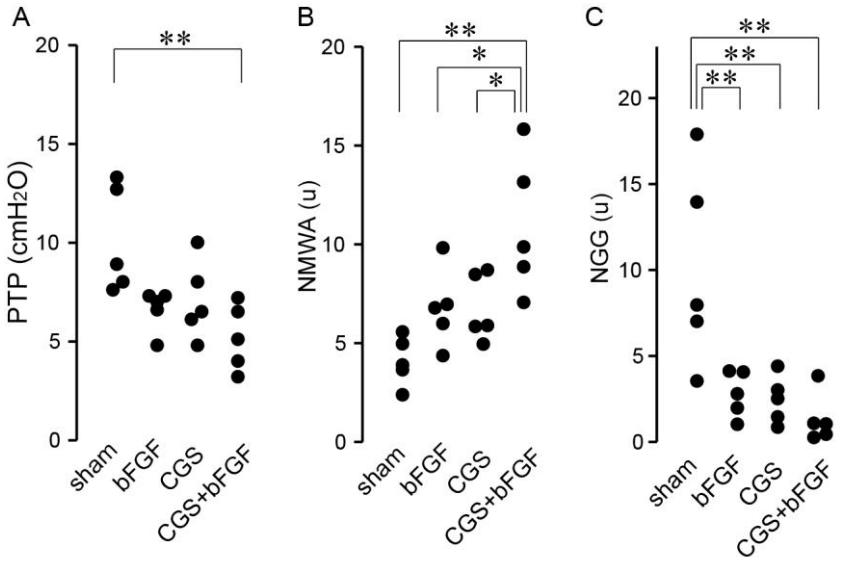

Figure 9 Supporting information

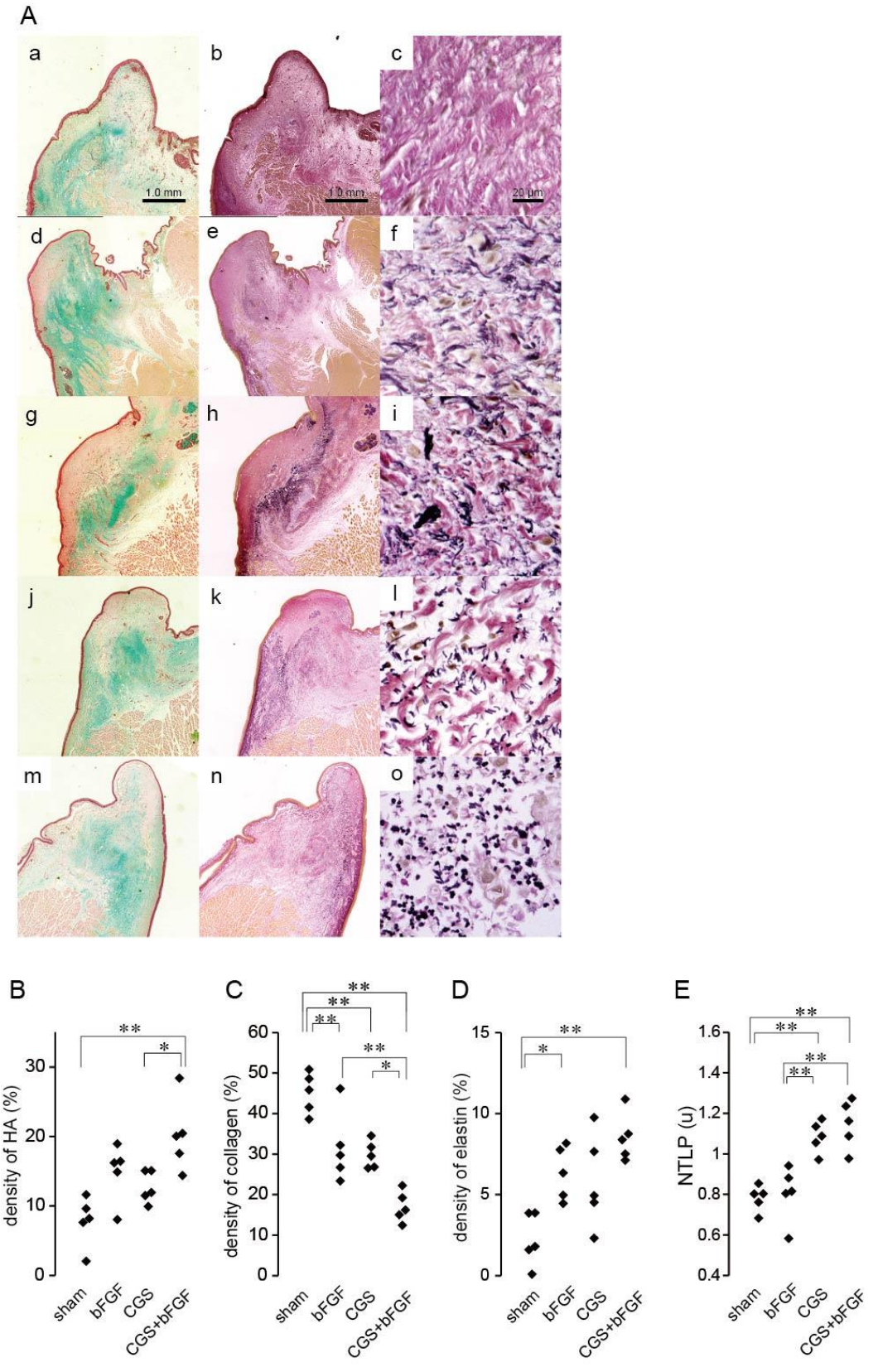

Figure Legends of Supporting Information

Table 2 SuppInfo.

Time course of bFGF retention on collagen/gelatin sponge under the condition of bFGF 100 ng/mL. Residual bFGF was analysed by ELISA. Data are expressed mean ± SD (n = 6).

Table 3 SuppInfo.

Time course of endogenous bFGF levels under the condition of bFGF 100 ng/mL. The culture media was harvested over time and analysed by ELISA. Data are expressed mean ± SD (n = 6).

Figure 8 SuppInfo.

Results of vibratory examinations. Data for all beagles in each group are plotted (each n=5). A) Phonation threshold pressure (PTP). B) Normalized mucosal wave amplitude (NMWA). C) Normalized glottal gap (NGG). $^{**}p < 0.01$, $^{*}p < 0.05$.

Figure 9 SuppInfo.

A) Representative images of histological examinations. Alcian blue staining (a, d, g, j, m) and elastica van Gieson staining (4x magnification: b, e, h, k, n; 40x magnification: c, f, i, l, o) of the sham-treated group (a, b, c), the bFGF group (d, e, f), the CGS group (g, h, i), the CGS + bFGF group (j, k, l) and the normal vocal fold (m, n, o). The CGS + bFGF group showed better hyaluronic acid restoration (blue stained area). Tissue contraction and dense collagen deposition was reduced in both implanted groups and reorganization of elastin were observed in the bFGF group and the CGS + bFGF group. B-E) Data for histological examination from all beagles in each group are plotted (each n=5). B) Density of hyaluronic acid. C) Density of dense collagen deposition. D) Density of elastin. E) Normalized thickness of the lamina propria (NTLP). $^{**}p < 0.01$, $^{*}p < 0.05$.